Chem. Senses 23: 385–395, 1998

Pheromone Deactivation Catalyzed by Receptor Molecules: a Quantitative Kinetic Model

Karl-Ernst Kaissling

Max-Planck-Institut für Verhaltensphysiologie Seewiesen, 82319 Starnberg, Germany

Correspondence to be sent to: Dr Karl-Ernst Kaissling, apl. Prof., Max-Planck-Institut für Verhaltensphysiologie Seewiesen, Postfach 1564, D-82305 Starnberg, Germany. e-mail: kaissling@mpi-seewiesen.mpg.de

Abstract

A quantitative model of pheromone–receptor interaction and pheromone deactivation, the supposed rate-limiting processes underlying the receptor potential kinetics, is worked out for the moth *Antheraea polyphemus*. In this model, the pheromone interacts with the receptor molecule while bound to the reduced form of the pheromone binding protein. The receptor molecules—besides their receptor function—catalyze the observed shift of the pheromone-binding protein from the reduced to the oxidized form (Ziegelberger, G., Eur. J. Biochem., 232, 706–711, 1995), which deactivates the pheromone bound to pheromone binding protein. With the following parameters, the model fits morphological, radiometric, electrophysiological and biochemical data: a maximum estimate of 1.7×10^7 receptor molecules/cell (with 40 000 units/μm^2 of receptor cell membrane), rate constants $k_1 = 0.2/(s \cdot \mu M)$ for the association, $k_2 = 10/s$ for the dissociation of the ternary complex of binding protein, pheromone and receptor, and $k_3 = 10/s$ for the deactivation via the redox shift. With these parameters, the duration of elementary receptor potentials elicited by single pheromone molecules (~50 ms) reflects the lifetime of the ternary complex, $\tau = 1/(k_2 + k_3)$. The receptor occupancy produced by the model for threshold stimuli fits the sensitivity of the receptor cell to single pheromone molecules.

Introduction

Insect olfactory hairs (sensilla trichodea) that adsorb pheromone molecules are chemoreceptor organs of the flux detector type, as opposed to concentration detectors (Kaissling, 1998). In the latter, the receptor cells are exposed to a stimulus concentration which is equal or proportional to the external stimulus concentration. Flux detectors such as sensilla trichodea of moth antennae accumulate stimulus molecules in a perireceptor compartment (Steinbrecht, 1992), and deactivate them after they have excited the receptor cell inside the hair. For moths, the postulate of a rapid stimulus deactivation in contrast to the slow enzymatic degradation detected by Kasang and co-workers (Kasang, 1971; Kasang *et al.*, 1988) was derived from the kinetics of the receptor potential (Kaissling, 1972). Evidence has since accumulated that the kinetics of the receptor potential mainly reflects the kinetics of extracellular processes (Kaissling, 1998) rather than the kinetics of cellular transduction processes (Breer *et al.*, 1994).

The concept of flux detectors has been discussed by means of kinetic models, including the association and dissociation of stimulus molecules and receptor molecules, and the stimulus deactivation (Kaissling, 1998). One version of these models used here corresponds to a simple enzymatic reaction scheme with the receptor molecules catalyzing the stimulus deactivation. The goal of the study is to apply this model to pheromone receptors of the moth *Antheraea polyphemus* and to determine a set of rate constants for the various processes which fit electrophysiological (Zack, 1979; Meng *et al.*, 1989), radiometric (Kanaujia and Kaissling, 1985; Kasang *et al.*, 1988; Kaissling, 1995b), biochemical (Vogt *et al.*, 1985; Ziegelberger, 1995) and morphometric data (Gnatzy *et al.*, 1984; Keil, 1984).

It seems possible to determine rate constants, although none of these processes can be measured directly, and pheromone receptor molecules have not yet been identified in insects. Most likely, however, specific receptor molecules are located within the dendritic plasma membrane. Since each of several receptor cells innervating a sensillum is tuned to a different pheromone component, specificity must be associated with the receptor cell.

Several specific properties of flux detectors facilitate their analysis (Kaissling, 1998). The rate of adsorption of stimulus molecules (stimulus uptake rate) is proportional to the external stimulus flux, the product of the external stimulus concentration and the relative velocity of the medium. At constant stimulus flux, a flow equilibrium can be reached, at which the rate of stimulus deactivation equals the uptake rate. Furthermore, at flow equilibrium, the number of receptor molecules occupied by stimulus molecules (receptor occupancy) is linearly proportional to

the uptake rate. The latter was determined using ^{3}H-labeled pheromone, here (*E,Z*)-6,11-hexadecadienyl acetate, the major pheromone component of *A. polyphemus* (Kaissling, 1987).

For the flow equilibrium, the relationship between receptor occupancy and receptor potential is given by the dose–response curve, in which the equilibrium amplitude of the receptor potential is plotted against the stimulus uptake. On the assumption that the receptor potential at any moment reflects the receptor occupancy, the decline of the occupancy after the end of stimulation and the rate of stimulus deactivation can be estimated.

Recently, a mechanism of pheromone deactivation was proposed which is based on the redox shift of the pheromone binding protein (PBP) observed in homogenates of olfactory hairs (Kaissling, 1995a; Ziegelberger, 1995). It has been suggested that the pheromone molecules entering the olfactory hair lumen are bound to the reduced form of the PBP (PBP_{red}), thus being solubilized (Van den Berg and Ziegelberger, 1991) and transported to the receptor cell. After exciting the receptor cell, the complex of pheromone (Ph) and PBP_{red} (Ph–PBP_{red}) turns into the oxidized form (Ph–PBP_{ox}), which is assumed not to be able to activate further receptor molecules. This redox shift might be catalyzed by the receptor molecules of the receptor cell membrane (Figure 1). The *in vitro* kinetics of this putative deactivation process will be compared with the rate constants determined for the *in situ* model.

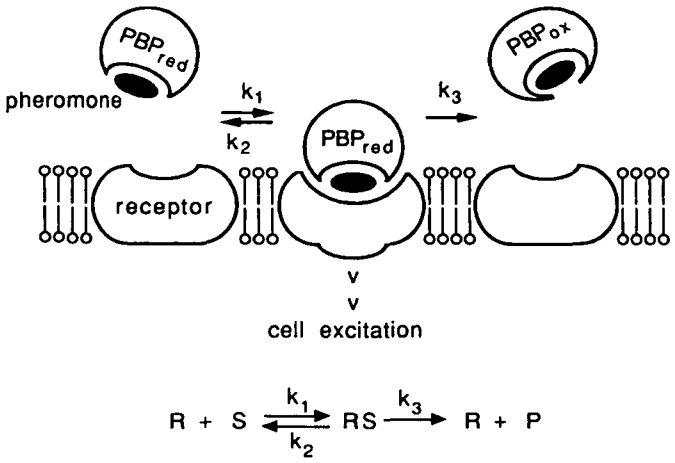

Figure 1 Schematic view of the hypothetical excitation–deactivation mechanism discussed. In the reaction scheme, *R* is the receptor molecule, *S* the complex of pheromone and the reduced form of the pheromone binding protein (Ph–PBP_{red}), and *P* the complex Ph–PBP_{ox}. *RS* is the ternary complex Ph–PBP_{red}–receptor which induces receptor cell excitation and the redox shift of the PBP, both involving conformational changes. Both the pheromone and the binding protein could interact directly with the receptor when the ternary complex Ph–PBP_{red}–receptor is formed. The PBP has six highly conserved cysteines (Raming *et al.*, 1989; reviewed in Pelosi, 1996) and one binding site for the pheromone (Du *et al.*, 1994). PBP_{red} has one or two, and PBP_{ox} has three S-S bridges (Ziegelberger, 1995). The conformational change of the PBP accompanying the observed redox shift might physically deactivate the pheromone.

The perireceptor events

Perireceptor events in moth pheromone sensilla comprise a number of processes (Kaissling, 1996), some of which will be neglected here if they appear to be of minor importance for the kinetics of the receptor potential.

1. Pheromone molecules adsorbed onto the olfactory hairs were shown to migrate along the hair and to enter the hair lumen. Most likely, the transport of the pheromone from the hair surface to the receptor cell by diffusion is not time limiting for the receptor potential. This inference is based on the diffusion coefficient (3×10^{-7} cm^2/s) determined for the longitudinal migration of tritium-labeled pheromone molecules on the sensory hair of *A.polyphemus* [Kanaujia and Kaissling, 1985; see also Steinbrecht (1973) for *Bombyx mori*]. Since this coefficient most likely also applies to the diffusion of stimulus molecules across the hair wall (via pores; see Steinbrecht, 1997) and through the sensillum lymph towards the receptor cell membrane, the transport time would, indeed, be negligible. According to a diffusion model developed by J. Thorson, Oxford (described in Kaissling, 1987), a much smaller diffusion coefficient would be expected (5×10^{-9} cm^2/s) if diffusion were rate limiting for the receptor potential. Thus, it can be assumed that the pheromone molecules are distributed on and within the hair in a negligible time.
2. Pheromone molecules entering the sensillum lymph in the hair lumen are bound to the PBP. With a dissociation constant of 60 nM (nmol/l) for the complex PBP–pheromone (Kaissling *et al.*, 1985) and a PBP concentration of 10 mM in the sensillum lymph (Vogt and Riddiford, 1981; Klein, 1987), only one out of 170 000 pheromone molecules at equilibrium is free (Kaissling, 1986, 1987). Since the number of pheromone molecules at physiological stimulus intensities is far below this value, and since single pheromone molecules per sensillum are sufficient to elicit responses, the pheromone bound to the protein most likely represents the effective stimulus S. For simplicity, it is assumed that the pheromone molecules entering the hair lumen are bound to the PBP within negligible time, predominantly to its reduced form because this form is most abundant in the sensillum lymph (80% of total PBP; Ziegelberger, 1995).
3. Binding of the effective stimulus to the receptor molecule. In the model, the complex Ph–PBP_{red} is considered as the stimulatory agent *S* which (reversibly) binds to the receptor molecule *R* and forms a complex *RS*. This latter complex is thought to trigger the cell response, i.e. to induce an increase of conductance of the receptor cell membrane for each *RS* formed.
4. Within the complex *RS*, *S* is converted to the product

P, the deactivated stimulus complex Ph–PBP_{ox}, which dissociates from R.

5. The complex Ph–PBP_{ox} may in turn dissociate, freeing the pheromone molecule, which may rebind to a PBP_{red} molecule and stimulate again. This effect could be responsible for the tailing of the receptor potential and, especially, of the nerve impulse response (Figure 5b; see also Kaissling, 1987, figure 37). Since the fraction of free pheromone molecules is very small compared with pheromone bound to PBP, dissociation and rebinding will be neglected here.
6. Finally, the free pheromone molecule may be enzymatically degraded by the sensillar esterase in the sensillum lymph. Although the purified esterase has a very rapid turnover (Vogt *et al.*, 1985), the pheromone degradation *in situ* takes minutes (Kasang *et al.*, 1988) and will be neglected here. The discrepancy is resolved if one assumes that the large proportion of pheromone bound to PBP (both forms) is protected from enzymatic degradation. This can be inferred from the study of Vogt and Riddiford (1986; see Kaissling, 1986).

The minor importance of enzymatic degradation for the rapid kinetics of the cell response was confirmed experimentally. Thus, the decline of the receptor potential within the first few seconds was practically unchanged in antennae, which, for unknown reasons, contained PBP but lacked >99% of the sensillar esterase (Maida *et al.*, 1995). Further support was given by experiments with inhibitors of the sensillar esterase which do not inhibit the decline of the receptor potential (B. Pophof, personal communication).

In conclusion, this paper is restricted to the processes involving the receptor molecules (3 and 4). An extended model including all of the processes listed above will be published elsewhere.

The model reaction system

The following reaction system of receptor occupancy and stimulus deactivation is discussed; it includes the adsorption of stimulus molecules on the olfactory hair (Kaissling, 1998).

$$S_{ext} \xrightarrow{a} S \qquad S + R \underset{k_2}{\overset{k_1}{\rightleftharpoons}} RS \xrightarrow{k_3} R + P$$

S_{ext} represents the external pheromone concentration. The factor a (/s) depends on the velocity of the external medium relative to the receptor organ, and on the geometry of the adsorptive structures and their adsorptive properties.

The product $a \cdot S_{ext}$ is equal to the adsorptive stimulus uptake rate U (concentration/s), which is defined here as the number of pheromone molecules adsorbed per second by a sensory hair, divided by the volume of the hair (2.6 pl). The number of adsorbed molecules per hair and per second has been calculated from measurements using ^{3}H-labeled pheromone molecules (Kanaujia and Kaissling, 1985; Kaissling, 1987, 1995b, 1996). At least half of the adsorbed molecules have been shown to enter the sensillum lymph space (Kanaujia and Kaissling, 1985); its volume is about half of the total hair volume.

S represents the effective stimulus concentration, i.e. the concentration of the complex Ph–PBP_{red}. For simplicity, S and all other reaction partners are assumed to be distributed over the entire volume of the hair. This seems adequate if diffusion of the pheromone within the hair is not a rate-limiting factor.

R represents, again for simplicity, a fictive concentration of (free) receptor molecules, i.e. their number (on the plasma membrane of the receptor cell dendrite) divided by the hair volume.

RS is the ternary complex Ph–PBP_{red}–receptor molecule, which induces the receptor cell response. Again, RS is considered as a concentration related to the hair volume. It is assumed that the electrical conductance of the receptor cell membrane increases in proportion to RS (Kaissling, 1974, 1977; Kodadová and Kaissling, 1996).

P denotes the deactivated pheromone, i.e. the inactive complex Ph–PBP_{ox}.

Note that the sum $S + RS + P$ is equal to the integral of adsorbed molecules during stimulation. The total number of receptors corresponds with

$$R_{tot} = R + RS \tag{1}$$

The terms k_1 [/(s·μM)], k_2 (/s) and k_3 (/s) are rate constants of association, dissociation and deactivation, respectively, as in the reaction scheme of a simple enzymatic process (Figure 1), with

$$K_m = (k_2 + k_3)/k_1 \tag{2}$$

At a constant rate of stimulus uptake U, and if $U < U_{sat}$, the concentrations of S and RS approach constant values (flow equilibrium, Figure 2).

Determination of model parameters: R_{tot} and k_3

For a flux detector, the product $k_3 \cdot R_{tot}$ can be determined from the dose–response relationship for receptor occupancy (Kaissling, 1998). For the equilibrium and with $RS < R_{tot}$, the rate of stimulus deactivation $k_3 \cdot RS$ equals the stimulus uptake rate U

$$k_3 \cdot RS = U \tag{3}$$

Considering the relative receptor occupancy, this relationship can be written as

$$RS/R_{tot} = U/(k_3 \cdot R_{tot}) \tag{4}$$

According to this equation, the receptor occupancy

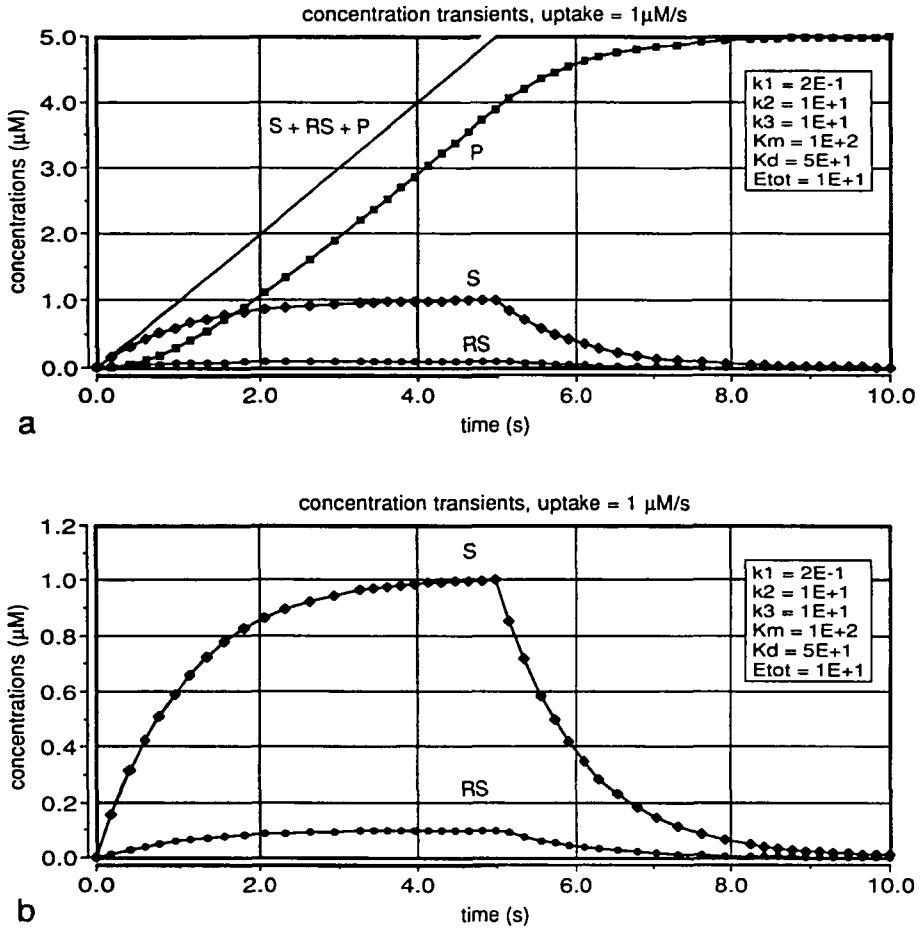

Figure 2 Time course of concentrations generated by a computer model (developed by J. Thorson, Oxford) of the reaction scheme discussed. **(a)** Concentrations of *S*, *RS*, *P* and their sum, which is equal to the total concentration of adsorbed stimulus molecules. **(b)** Concentrations of *S* and *RS*, same as in (a), but expanded ordinate scale. Constant rate of stimulus uptake *U* between 0 and 5 s. The following parameters were used: U = 1 μM/s, R_{tot} = 10 μM, K_m = 100 μM, k_3 = 10/s, k_2 = 10/s, k_1 = 0.2/(μM · s) (see Figure 7, parameter set 1a). The model produced a half-time of 0.79 s for the decline of *RS* following stimulation, a value within the lower range of values derived from experimental data (0.5–2 s; Figures 4 and 5).

RS/R_{tot} increases linearly until the rate of uptake equals the maximum velocity of deactivation $k_3 \cdot R_{tot}$. The 'just-saturating' uptake rate is

$$U_{sat} = k_3 \cdot R_{tot} \quad (5)$$

At uptake rates above U_{sat}, the receptor occupancy is maximal, but no equilibrium concentration of S can be obtained.

A minimum value of U_{sat} may be determined assuming that the receptors cannot be fully occupied before the receptor potential saturates. According to this consideration, the curve of receptor occupancy versus stimulus uptake rate is placed with U_{sat} just above the stimulus uptake for the highest receptor potential amplitude (Figure 3). The uptake was calibrated using ^{3}H-labeled (*E,Z*)-6,11-hexadecadienyl acetate (Kaissling, 1987, 1995). For the averaged dose–response curve of the receptor potential amplitudes measured in *A.polyphemus* (Zack, 1979), U_{sat} must be >40 μM/s, the highest uptake rate tested in the electrophysiological experiment. The dose–response curve of the receptor potential has a slope covering many decades of stimulus uptake and does not reach full saturation at the highest stimulus intensities applied. Therefore, for all further calculations, the just-saturating uptake rate U_{sat} is set somewhat higher, to 100 μM/s, which means that the minimum value of $k_3 \cdot R_{tot}$ = 100 μM/s (equation 5).

For R_{tot}, one can calculate a maximum value based on the assumption that the receptor molecules are about as tightly packed in the dendritic receptor cell membrane as the rhodopsin molecules in the disk membrane of visual cells (Dratz and Hargrave, 1983). With a maximum estimate of 40 000 units/μm^2 and an area of the outer segment of receptor cell dendrite of 426 μm^2 (Keil, 1984; for identification of the cell, see Kumar and Keil, 1996), we obtain 1.7 × 10^7 receptor molecules/dendrite; this reveals a fictive concentration of R_{tot} = 10.9 μM in the hair volume of 2.6 pl. In the following, R_{tot} is rounded to 10 μM. With this

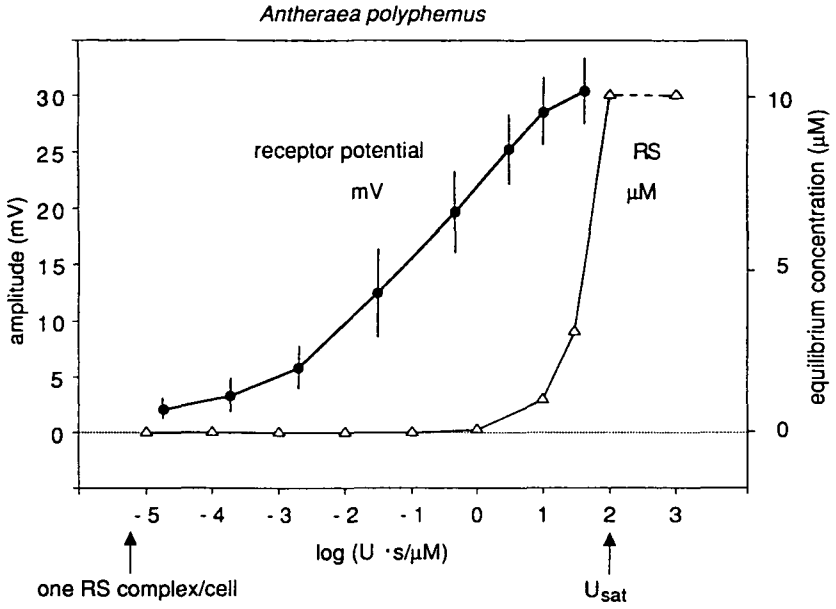

Figure 3 Dose–response relationships of receptor potential and receptor occupancy. The abscissa gives the log stimulus uptake U of ^{3}H-labeled (*E,Z*)-6,11-hexadecadienyl acetate by the sensilla trichodea (molecules adsorbed per second and per total hair volume, given in μM/s) (Kaissling *et al.*, 1987). Dots: receptor potential amplitudes (mV ± SD, left ordinate) measured after 2 s of stimulation and averaged from 15 hair sensilla (Zack, 1979). Triangles: theoretical equilibrium concentrations of the stimulus–receptor complex *RS* (in μM, right ordinate), which are linearly related to U (equation 3). This curve was placed such that the just-saturating stimulus uptake rate U_{sat} (arrow, right hand) was above the highest rate used for measuring the receptor potential. The maximum value of *RS* (R_{tot} = 10 μM) corresponds to a maximum number of 1.7×10^7 receptor molecules/receptor cell (see Figure 7). The theoretical equilibrium value of one *RS* complex per cell would be reached at an uptake rate = $U_{sat}/(1.7 \times 10^7)$, indicated by the left-hand arrow. This rate of uptake corresponds to an adsorption rate of 10 molecules/(hair · s).

figure and according to equation (5), the rate constant of the stimulus deactivation would be $k_3 = U_{sat}/R_{tot} = 100$ μM/(s · 10 μM) = 10/s.

Determination of model parameters: K_m

Considering the model of pheromone–receptor interaction as a simple enzymatic system, its $K_m = (k_2 + k_3)/k_1$ can be determined from $U_{sat} = k_3 \cdot R_{tot}$ (equation 6) and from k_{RS}, the rate constant of the decline of *RS* after the end of stimulus exposure, i.e. when S_{ext} is set to zero (Figure 2). After weak stimuli with $S << K_m$ and given $R_{tot} << K_m$, the concentration *RS* declines as an exponential process with an approximate rate constant k_{RS} (from Kaissling, 1998)

$$k_{RS} = -\mathrm{d}RS/(\mathrm{d}t \cdot RS) \approx k_3 \cdot R_{tot}/K_m \qquad (6)$$

The rate of decline of *RS* can be estimated from the decline of the receptor potential, given that the amplitude of the latter is related to the actual concentration *RS* during the decline in the same way as at flow equilibrium. At equilibrium, the receptor potential amplitude is related to the concentration *RS*, as indicated by the dose–response curve (see Introduction). To construct this curve (Figure 4a), the receptor potential amplitudes were measured at the end of a 2 s stimulus, when a steady state was approximated (Zack, 1979). Using the time of half-decline of the receptor potential after termination of stimulus exposure (Figure 4b) given by Zack (1979), one obtains a half-life of *RS* ($t_{RS1/2}$) between 0.5 and 2 s, depending on the stimulus intensity (Figure 4d).

In a different experiment, the conversion of the receptor potential amplitudes into relative concentrations of *RS* is shown for the decline of the receptor potential (Figure 5). Six examples of receptor potentials recorded from a single sensillum are given (Figure 5a, b). The graphs show responses to three stimuli of each of two unknown, but strongly different pheromone concentrations with the durations 20 ms, 200 ms and 2 s. Since the release rates of pheromone for the type of odor sources used here have been shown to be independent of stimulus duration (Kodadová, 1996), the relative amounts of pheromone released by each odor source were ~1:10:100. For the two strongest stimuli (Figure 5b), the decline starts with some delay, probably due to overloading of the hairs with stimulus molecules indicating oversaturation of the deactivation process.

By means of the measured dose–response curve (Figure 4a), the receptor potential amplitudes of the six responses were converted into relative concentrations of *RS*, which are proportional to the relative uptake rate $U_{rel} = U/U_{sat}$ (equations 4 and 5). The decline of *RS* obtained by the four weaker of the six stimuli was found to be exponential with a half-time of decline of about $t_{RS1/2} = 0.5$ s over a wide range of stimulus intensities (Figure 5c). The decline following the two strongest of the six stimuli was slower, with $t_{RS1/2}$ of

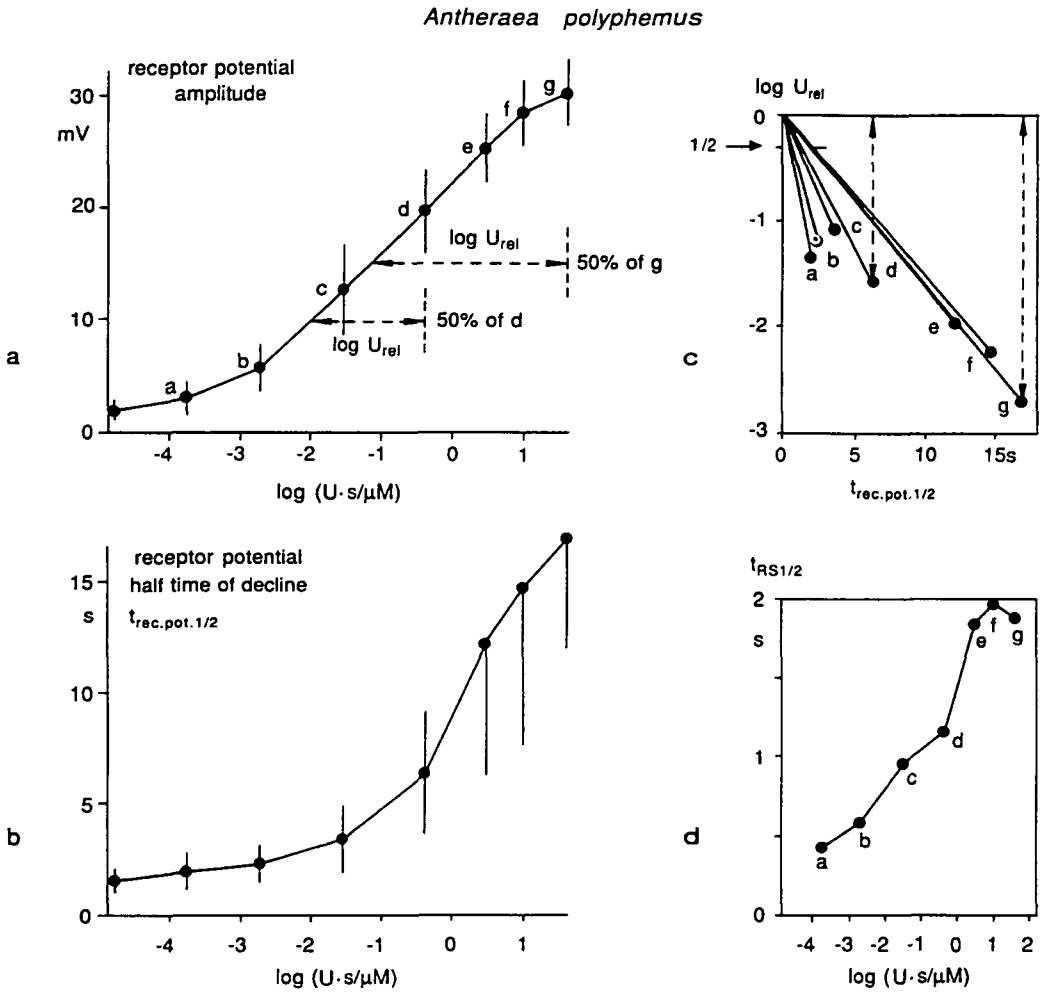

Figure 4 Apparent half-life of the excitatory complex *RS* ($t_{RS1/2}$) as determined from the dose–response curve of the receptor potential [**(a)**, same curve as in Figure 3] and its half-time of decline ($t_{rec.pot.1/2}$) **(b)**. It is assumed that the relationship between receptor occupancy *RS* and the receptor potential amplitude is the same for both the equilibrium (Figure 3) and the decline of the receptor potential. For each of the amplitudes a–g (a), the rate of stimulus uptake *U* (μM/s) was related to the rate *U* producing half of the respective amplitude. The log of this ratio (log U_{rel}) is indicated for g and d by lengths of the dashed lines. The values of log U_{rel} are plotted in **(c)** against the half-times of receptor potential decline ($t_{rec.pot.1/2}$) taken from (b) (Zack, 1979). Since *RS* is proportional to *U* (equation 3), the straight lines in (c) represent the apparent exponential decline of *RS* (see Figure 5c). From the diagram in (c), the apparent half-lives of *RS* ($t_{RS1/2}$) were taken (at U_{rel} = 1/2); they are plotted against log *U* in **(d)**.

~2 s. From $t_{RS1/2}$ = 0.5 s, fitting the lower value of the half-times of the decline of *RS* obtained in both experiments (Figures 4 and 5), we calculate a rate constant k_{RS} = 1.4/s by using

$$k_{RS} = -\mathrm{d}RS/(\mathrm{d}t \cdot RS) = \ln 2/t_{RS1/2} \qquad (7)$$

With this rate constant and the product $k_3 \cdot R_{tot}$ = 100 μM/s obtained from the saturating stimulus uptake U_{sat} (Figure 3), one finds, according to equation (6), K_m = 72 μM:

$$K_m \approx k_3 \cdot R_{tot}/k_{RS} \qquad (8)$$

We use a rounded value of K_m = 100 μM which corresponds to $t_{RS1/2}$ = 0.693 s (or k_{RS} = 1/s), which is still in the lower range of the measured half-times (0.5–2 s). Equation (8) shows that the value determined for K_m depends on the product $k_3 \cdot R_{tot}$ obtained from the dose–response curve, and on the decline of *RS* deduced from the decline of the receptor potential.

Figure 2 demonstrates the transients of *S*, *RS* and *P* generated by a computer model (developed by J. Thorson, Oxford) with the above values of R_{tot} = 10 μM, k_3 = 10/s and K_m = 100 μM for a small rate of stimulus uptake *U* = 1 μM/s, which provides the condition $S << K_m$. However, with R_{tot} = 10 μM and K_m = 100 μM, the condition $R_{tot} << K_m$ is not exactly fulfilled. As a result, the approximation of equation (6) is not quite correct; the half-time given by the model for the decline of *RS* is 0.79 s, slightly deviating from 0.693 s obtained from equation (8).

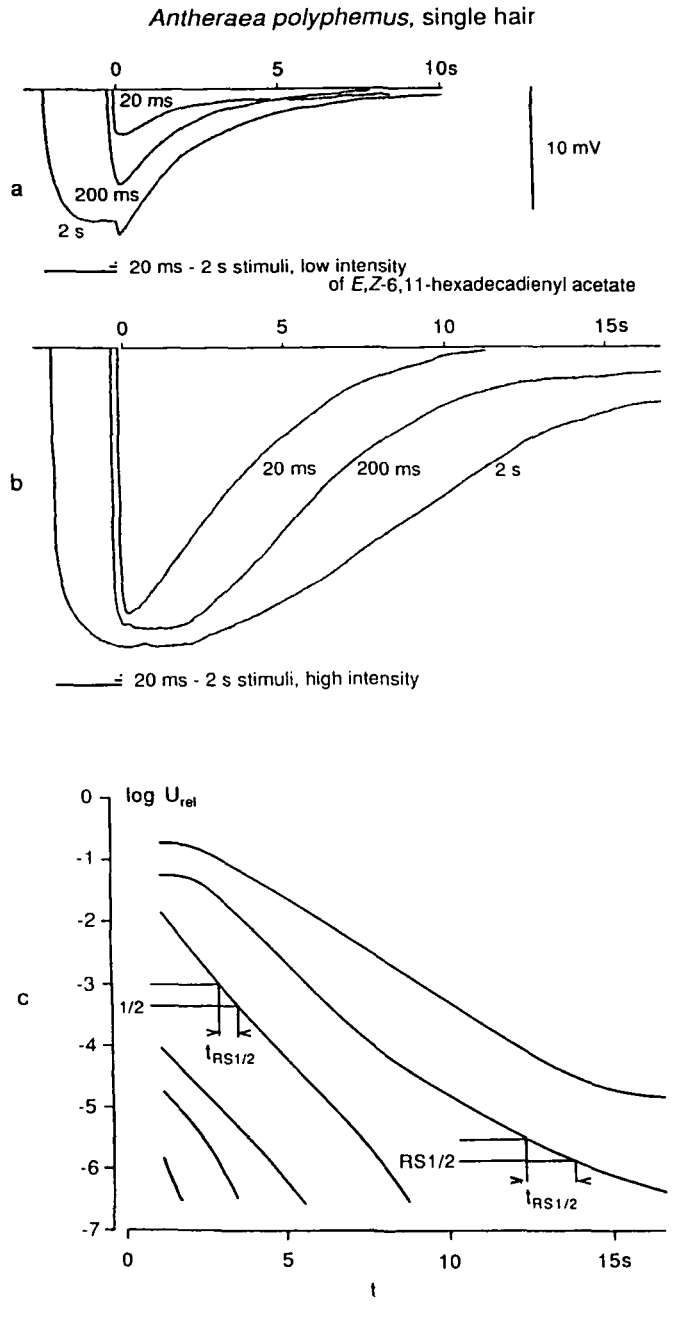

Figure 5 Decline of U_{rel} (here = U/U_{max}) as determined from the decline of six receptor potentials **(c)**. The receptor potentials **(a, b)** were produced with a medium stimulus intensity (a) and a very strong stimulus intensity (b), with stimulus durations of 20 ms, 200 ms and 2 s. The two strongest of the six responses show an initial plateau suggesting oversaturation (possibly due to $U > k_3 \cdot R_{tot}$). Time zero is the end of stimulation for all recordings, same time scale for (a–c). The receptor potential amplitudes were converted into values of U_{rel} using the (averaged) dose–response curve shown in Figure 3. U_{max} corresponds to the uptake for the highest response amplitude of the dose–response curve. U_{rel} declines with an exponential time course (with $t_{RS1/2}$ of ~0.5 s) for the four weaker of the six responses (c). According to equation (3), *RS* is proportional to *U* and consequently also declines exponentially ($t_{RS1/2}$ of ~0.5 s). The slower decline observed in the two strongest of the six responses ($t_{RS1/2}$ of ~2 s) is not expected from the present model of stimulus deactivation.

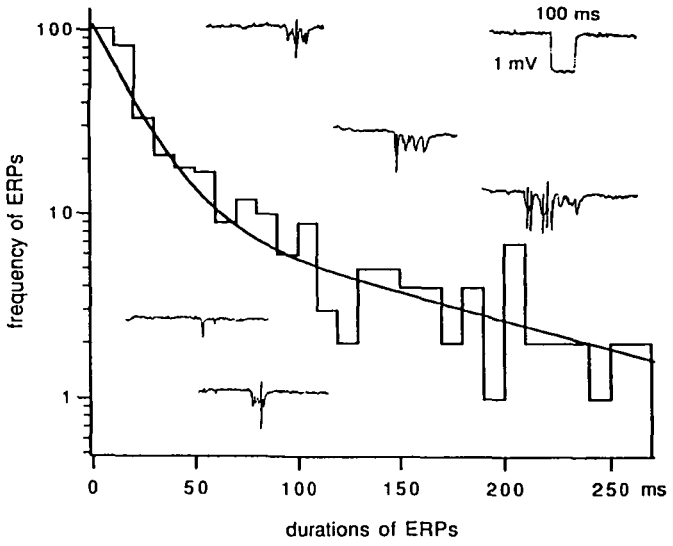

Figure 6 Frequency of occurrence (ordinate) of durations (abscissa) of n = 384 elementary receptor potentials (ERPs) produced by a bombykal receptor cell of *Bombyx mori* upon weak stimulation by bombykal (single-sensillum recording). Examples of ERPs (most of them followed by one or a few nerve impulses) and calibration are given. ERPs of relatively long duration fluctuate in amplitude. The distribution of ERP durations was fitted (by A. Redkozubov, Cernogolovka) to the sum of two exponentials with τ_1 = 18.7 ms (92%) and τ_2 = 158 ms (8%).

Determination of model parameters: k_2 and k_1

Further experimental data have been used in order to estimate the rate constants k_2 and k_1. Tentatively, it is assumed that the lifetime τ of the *RS* complex

$$\tau = 1/(k_2 + k_3) \qquad (9)$$

is reflected in the duration of the elementary receptor potentials (ERP). These transient potential changes can be elicited by a single pheromone molecule (see Kaissling and Thorson, 1980; Kaissling, 1994) and might be generated by an activation of a single receptor molecule. The durations of ~90% of these events follow a single exponential distribution, shown here for ERPs recorded from a pheromone receptor cell of the male silkmoth *B.mori* (Figure 6).

The ERPs were measured during stimulation with a low concentration of pheromone (bombykal), chosen such that the mean ERP duration was ~1% of the mean intervals of quiet baseline between ERPs. The ERPs of longer duration usually appear as bursts of irregular fluctuations (Figure 6, insets). Their duration was taken as the time interval from the beginning to the end of the burst. The distribution shown in Figure 6 is consistent with the sum of two exponentials. The shorter time constant determined for most of the events was τ = 20 ms. For our consideration of the reaction scheme for *A.polyphemus*, we use a preliminary value of τ = 50 ms (K.-E. Kaissling, unpublished measurements). With k_3 = 10/s, we obtain k_2 = 10/s [equation (9)].

Using equation (2), one can now calculate $k_1 = 0.2/(s \cdot \mu M)$ (Figure 7, parameter set 1a). The values of k_1 and k_2 calculated for $\tau = 20$ ms and $\tau = 90$ ms are given in Figure 7, sets 1b and 1c, respectively.

Discussion

Diffusion does not control the stimulus–receptor association

The value of k_1 indicates whether the stimulus–receptor association is controlled by diffusion or by other processes. The values of k_1 expected for a diffusion-controlled process can be estimated using the equation given by von Smoluchowsky (1916; see Adam *et al.*, 1988):

$$k_{diff} = L4\pi r_{AB}(D_A + D_B) \qquad (10)$$

L is the Loschmidt number (6.023×10^{23} molecules/mol), r_{AB} is the reaction distance (0.5 nm), and $D_A + D_B$ are the diffusion coefficients of the reaction partners. As a diffusion coefficient of the pheromone, we use 3×10^{-7} cm^2/s, the value determined for the longitudinal transport along the sensillum (Kanaujia and Kaissling, 1985). With respect to the size of the PBP (15 kDa), this value is compatible with diffusion of the complex Ph–PBP in the sensillum lymph (Adam *et al.*, 1988). The diffusion coefficient of the second partner, the receptor molecules at the cell membrane, is thought to be much smaller and, thus, neglected. Using these numbers, one obtains a theoretical value of k_1 of ~200/(s · μM) for a diffusion-controlled formation of RS.

The values of k_1 determined here are far below those for a diffusion-controlled process. For a given K_m, the value of k_1 depends on τ. For the τ values between 20 and 90 ms, the corresponding values of k_1 are between 0.5/(s · μM) and 0.1/(s · μM) (Figure 7, parameter sets 1b and 1c). These values of k_1 are much smaller than k_{diff}, which suggests that slower processes than diffusion are rate limiting for the interaction of S and R. Whether the binding of the complex Ph–PBP$_{red}$ to the receptor is the time-consuming process or whether other so far neglected processes are limiting, for instance the binding of the pheromone to the PBP, needs further analysis.

The significance of the rate constants for the cell response

Interestingly, in the present model of a flux detector, at flow equilibrium, the rate constants k_1 and k_2 have no influence on the receptor occupancy (and consequently on the response amplitude) which depends on k_3 and RS only [equation (3)]. Furthermore, according to equation (6), valid for $S << K_m$ and $R_{tot} << K_m$, the rate constants k_2 and k_3 do not influence k_{RS} if $k_3 >> k_2$. In this case, k_{RS}, governing the decline of the receptor potential, depends on the product $k_1 \cdot R_{tot}$ only. However, if $k_3 << k_2$, we find

$$k_{RS} = k_1 \cdot R_{tot} \cdot k_3/k_2 \qquad (11)$$

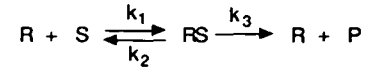

parameter set	1a	1b	1c	2	
U_{sat}	100				μM/s
R_{tot}	10			5	μM
k_3	10			20	/s
k_{RS}	1				/s
K_m	100			100	μM
τ	50	20	91	48	ms
k_2	10	40	1	1	/s
k_1	0.2	0.5	0.11	0.21	/(s · μM)
K_d	50	80	9	4.8	μM

Figure 7 Sets of model parameters obtained from the dose–response curve of the receptor potential ($U_{sat} = k_3 \cdot R_{tot}$), from its decline ($k_{RS} = k_3 \cdot R_{tot}/K_m$) and from the duration of elementary receptor potentials [$\tau = 1/(k_2 + k_3)$] (underlined values derived from electrophysiological measurements). The value of $R_{tot} = 10$ μM (parameter sets 1a–c) corresponds to a maximum density of receptor molecules similar to the that of rhodopsin in the disk membrane (40 000 units/μm^2), a dendritic membrane area of 426 μm^2 and a hair volume of 2.6 pl. The maximum number of receptor molecules per cell is $40\,000 \times 426 = 1.7 \times 10^7$. Parameter sets 1a–c demonstrate the dependence of k_1, k_2 and K_d ($= k_2/k_1$) on the value of τ, when R_{tot}, k_3 and K_m are unchanged. Parameter set 2 has a smaller R_{tot} compared with set 1a, but fits the data (U_{sat}, k_{RS} and τ) as well.

which means that, in this case, all three of the rate constants influence the receptor potential decline (Kaissling, 1998).

The latter condition applies for parameter set 1b only (Figure 7). In the other cases, we have $k_3 = k_2$ (set 1a) or $k_3 > k_2$ (sets 1c, 2) which means that changes in the decline time must be due to changes in k_1. Pheromone derivatives produce smaller receptor potentials than the pheromone, with characteristic compound-specific decline times (Kaissling, 1977, 1998). As observed within several species of moths, these decline times are mostly shorter than those of the pheromone responses, possibly due to higher k_1 or, in the case $k_3 << k_2$, also due to higher k_3 or smaller k_2 (equation 11). However, definite conclusions about the rate constants of interactions with pheromone derivatives cannot yet be drawn.

The total number of receptor molecules

Since R_{tot} is derived from a maximum assumption, an alternative set of parameters (Figure 7, parameter set 2) with the same K_m but a 2-fold smaller R_{tot} is given. In order to keep the maximum deactivation rate $k_3 \cdot R_{tot}$ equal to 100 μM/s, the value of k_3 had to be doubled. Correspondingly, the value of k_2 was decreased in order to keep the lifetime of the complex RS near to 50 ms. Both sets of parameters (1a and 2) fit the data obtained from dose dependence of the

receptor potential, its decline and the duration of ERPs. However, if R_{tot} were >2-fold smaller, k_3 would have to be increased even further, in order to keep $k_3 \cdot R_{tot} = 100\ \mu M/s$. This means that the lifetime $1/\tau$ of the ternary complex Ph–PBP–receptor (*RS*) would become shorter than the duration of the elementary receptor potentials.

Threshold considerations

The model parameters proposed (Figure 7, set 1a) are based on U_{sat}, on the decline of the receptor potential, on the duration of ERPs and on a maximum density of receptor molecules. It can be asked whether this model shows reasonable responses for stimulus intensities near threshold. At an uptake rate of 10 pheromone molecules per second and per cell (Figure 3, arrow, left-hand side) the model produces an (average) equilibrium occupancy of one *RS* complex per receptor cell (as can be deduced using equation 3). The complexes (with a lifetime of 50 ms) are formed at a rate of ~20 times per second and per cell. The above uptake rate is obtained at a stimulus intensity ~3-fold below the lowest intensity used in the electrophysiological recordings (Figure 3); according to extrapolation of the data of Zack (1979), it elicits ~10 nerve impulses per second and per cell. At this low impulse frequency each nerve impulse is preceded by an ERP, the first response of the receptor cell to a single pheromone molecule (Kaissling, 1994), which means that ~10 ERPs are formed per second and per cell. Thus, the ERPs compared with the *RS* complexes of the model are formed at a somewhat slower rate. In conclusion, satisfactory agreement between model and data is obtained; the model covers the entire working range of the receptor cell with respect to stimulus intensities. For a more appropriate analysis of the threshold situation the stochastic nature of weak stimuli needs to be considered.

Dissociation constants of pheromone–PBP binding and of stimulus–receptor interaction

It seems noteworthy that the binding affinity of pheromone and PBP is much higher (dissociation constant = 60 nM, Kaissling *et al.*, 1985; = 640 nM, Du and Prestwich, 1995) than the proposed affinity of the stimulus (Ph–PBP) and the receptor (K_d = 50 μM; Figure 7, data set 1a). This shows that high sensitivity of a chemoreceptor organ to single pheromone molecules does not necessarily involve high binding affinity between stimulus and receptor molecules. A similar situation applies for the reception of maltose in *Escherichia coli*. The maltose-binding protein (MBP) occurs in a high concentration (1 mM) in the periplasmic space; maltose is bound to the MBP with a K_d of 3 μM; the complex of MBP and maltose is bound to the receptor at the cell membrane less strongly, with a K_d of 250 μM (Manson *et al.*, 1985; Bohl *et al.*, 1995).

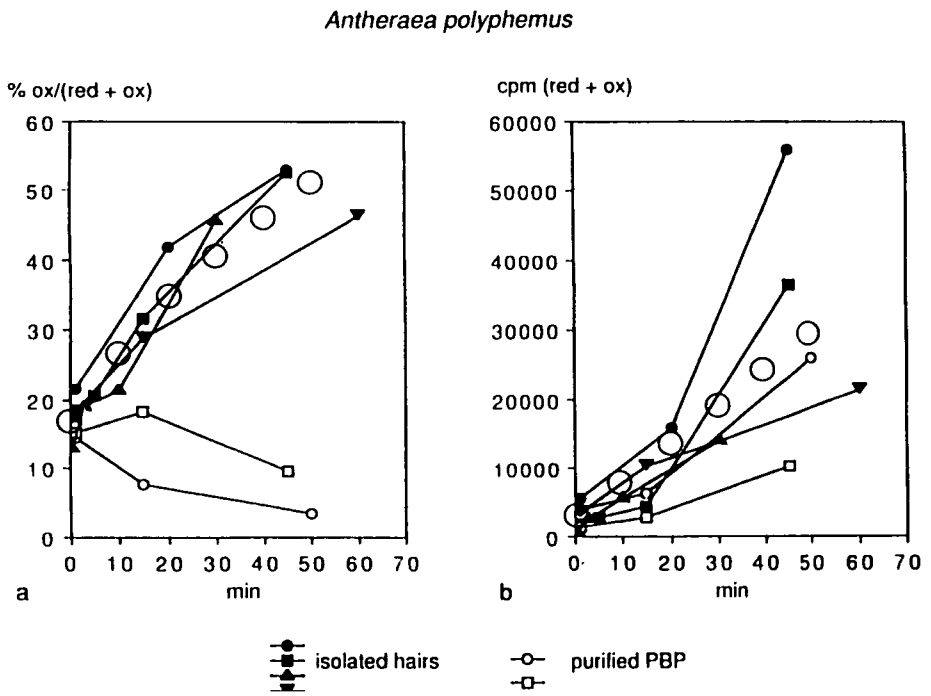

Figure 8 **(a)** Redox shift of pheromone-binding protein (PBP) *in vitro* followed by binding of ^{3}H-labeled (*E,Z*)-6,11-hexadecadienyl acetate to the oxidized (ox) and reduced (red) form of the PBP. The percentage of oxidized PBP increases with incubation time in isolated hair homogenates (filled symbols), but does not increase with purified PBP in buffer solution (open symbols). **(b)** The total amount of [^{3}H]pheromone bound to PBP increased with incubation time, due to a gradual release of the pheromone from the glass wall (from Ziegelberger, 1995). Large circles in (a) and (b) show the averaged transients used in the computer simulation.

Deactivation *in situ* and redox shift *in vitro*

We now consider whether the redox shift of the PBP observed *in vitro* (Ziegelberger, 1995) can serve as a deactivation mechanism although its velocity measured in the hair homogenate is much lower than that estimated from the receptor potential decline (Figure 8a). Since our reaction scheme represents an enzymatic process, an ~200-fold lower velocity is expected *in vitro* because the enzyme (= receptor) concentration in the homogenate is lower than in the hair by this factor. This extrapolation is possible if $R_{tot} << K_m$, under which condition the rate of the enzymatic degradation (k_{RS}) depends on the concentration of the enzyme (Kaissling, 1998). This condition is approximately fulfilled *in situ*, and even more so *in vitro* due to the high dilution factor. For the computer modeling of the *in vitro* experiment, it has also been taken into account that the pheromone concentration in the homogenate increased during incubation due to the gradual release of the pheromone from the glass wall (Figure 8b).

However, if the dilution factor of 200 is taken into account, the redox shift of the PBP observed *in vitro* proceeds more slowly than estimated from the model parameters. To simulate the redox shift *in vitro*, the enzyme concentration has to be lowered to 0.0038 μM, which is 7.6% of the value expected from the 200-fold dilution. Possibly, in the homogenate >90% of the receptor molecules had lost their catalytic ability.

Final remarks

Certainly, the model parameters have to be considered as preliminary. They might, for instance, change after including in the model other extracellular processes such as diffusional transport of the pheromone, its binding to the PBP and its enzymatic degradation. Furthermore, the parameters determined so far depend on the assumption that the relationship between receptor occupancy and amplitude of the receptor potential is the same during equilibrium and transients of the receptor potential. This first approach allowed hypotheses to be suggested about the number of receptor molecules, their possible catalytic function, the strength of binding to the receptor and the relationship between the duration of the elementary receptor potentials and the lifetime of the stimulus–receptor complex.

Although the model of stimulus deactivation discussed here is compatible with morphological, electrophysiological, radiometric and biochemical data, alternative models might be found. One alternative model could employ a separate enzyme to catalyze deactivation (Kaissling, 1998). However, the advantage of a mechanism in which receptor molecules serve as deactivating enzymes would be its one-way character: the pheromone molecules are not deactivated before they interact with a receptor molecule. This would guarantee maximum sensitivity of the receptor cells on the moth antennae, which obviously are designed for optimal molecule capture in view of their construction and enormous size (Kanaujia and Kaissling, 1985; Kaissling, 1987).

Many chemoreceptor organs which adsorb and do not desorb stimulus molecules during stimulus exposure (flux detectors; see Kaissling, 1998) might have a mechanism for rapid stimulus deactivation or removal. One of these organs may well be the vertebrate nose. Odor-degrading or odor-modifying enzymes have been found in the olfactory mucus (for references, see Pelosi, 1996), but it remains to be shown whether they deactivate the odor molecules rapidly enough or whether other processes serve this function. Whether odorant binding proteins (containing two cysteines only) are involved in stimulus deactivation in vertebrates is another challenging question.

Acknowledgements

I thank J. Thorson and A. Biederman-Thorson, Oxford, for programming a computer model of the reaction system, for helpful discussions and for linguistic help. I am very grateful to A. Redkozubov, Chernogolovka, Russia, for help in data evaluation and to A. Minor, Moscow, J.P. Rospars, Versailles, G. Stange, Canberra, A. Vermeulen, Versailles, B. Pophof, R.A. Steinbrecht, G. Ziegelberger and J. Ziesmann, Seewiesen, for valuable suggestions and comments on the manuscript. For technical help, I thank A. Günzel, U. Lauterfeld and C. Schmid.

References

Adam, G., Läuger, P. and **Stark, G.** (1988) Physikalische Chemie und Biophysik. 2. Aufl. Springer Verlag, Berlin, p. 399.

Bohl, E., Shuman, H.A. and **Boos, W.** (1995) *Mathematical treatment of the kinetics of binding protein dependent transport systems reveals that both the substrate loaded and unloaded binding proteins interact with the membrane components*. J. Theor. Biol., 172, 83–94.

Breer, H., Raming, K. and **Krieger, J.** (1994) *Signal recognition and transduction in olfactory neurons*. Biochim. Biophys. Acta: Mol. Cell Res., 1224, 277–287.

Dratz, E.A. and **Hargrave, P.A.** (1993) *The structure of rhodopsin and the rod outer segment disk membrane*. Trends Biochem. Sci., 8, 128.

Du, G.H. and **Prestwich, G.D.** (1995) *Protein structure encodes the ligand binding specificity in pheromone binding proteins*. Biochemistry, 34, 8726–8732.

Du, G.H., Ng, Ch.-Sh. and **Prestwich, G.D.** (1994) *Odorant binding by a pheromone binding protein: active site mapping by photoaffinity labeling*. Biochemistry, 33, 4812–4819.

Gnatzy, W., Mohren, W. and **Steinbrecht, R.A.** (1984) *Pheromone receptors in* Bombyx mori *and* Antheraea pernyi. *II. Morphometric analysis*. Cell Tissue Res., 235, 35–42.

Kaissling, K.E. (1972) *Kinetic studies of transduction in olfactory receptors of* Bombyx mori. In Schneider, D. (ed.), International Symposium on Olfaction and Taste IV. Wiss. Verlagsgesellschaft, Stuttgart, pp. 207–213.

Kaissling, K.E. (1974) *Sensory transduction in insect olfactory receptors*. In

Jaenicke, L. (ed.), Biochemistry of Sensory Functions. 25. Mosbacher Coll. Ges. Biolog. Chemie, Springer Verlag, Berlin, pp. 243–273.

Kaissling, K.E. (1977) *Structures of odour molecules and multiple activities of receptor cells.* In Le Magnen J. and MacLeod P. (eds), International Symposium on Olfaction and Taste VI. Information Retrieval, London, pp. 9–16.

Kaissling, K.E. (1986) *Chemo-electrical transduction in insect olfactory receptors.* Annu. Rev. Neurosci., 9, 121–145.

Kaissling, K.E. (1987) R.H. Wright Lectures on Insect Olfaction. Colbow, K. (ed.), Simon Fraser University, Burnaby, B.C., Canada, pp. 1–190.

Kaissling, K.E. (1994) *Elementary receptor potentials of insect olfactory cells.* In Kurihara K., Suzuki N. and Ogawa H. (eds), XI International Symposium on Olfaction and Taste. Springer Verlag, Tokyo, pp. 812–815.

Kaissling, K.E. (1995a) *Receptor mediated change of pheromone binding protein in* Antheraea polyphemus. ECRO XI. Chem. Senses, 20, 110.

Kaissling, K.-E. (1995b) *Single unit and electroantennogram recordings in insect olfactory organs.* In Spielman, A.I. and Brand, J.G. (eds), Experimental Cell Biology of Taste and Olfaction: Current Techniques and Protocols. CRC Press, Boca Raton, FL, pp. 361–386.

Kaissling, K.E. (1996) *Peripheral mechanisms of pheromone reception in moths.* Chem. Senses, 21, 257–268.

Kaissling, K.E. (1998) *Flux detectors versus concentration detectors: two types of chemoreceptors*. Chem. Senses, 23, 99–111.

Kaissling, K.E. and **Thorson, J.** (1980) *Insect olfactory sensilla: structural, chemical and electrical aspects of the functional organisation.* In Sattelle, D.B., Hall, L.M. and Hildebrand, J.G. (eds), Receptors for Neurotransmitters, Hormones and Pheromones in Insects. Elsevier/North-Holland Biomedical Press, Amsterdam, pp. 261–282.

Kaissling, K.E., Klein, U., de Kramer, J.J., Keil, T.A., Kanaujia, S. and **Hemberger J.** (1985) *Insect olfactory cells: electrophysiological and biochemical studies.* In Changeux, J.P. and Hucho, F. (eds), Molecular Basis of Nerve Activity. Proceedings of the International Symposium in Memory of D. Nachmansohn (Oct.1984), Berlin, New York, pp. 173–183.

Kanaujia, S. and **Kaissling, K.E.** (1985) *Interactions of pheromone with moth antennae: adsorption, desorption and transport*. J. Insect Physiol., 31, 71–81.

Kasang, G. (1971) *Bombykol reception and metabolism on the antennae of the silkmoth* Bombyx mori. In Ohloff, G. and Thomas, A.F. (eds), Gustation and Olfaction. Academic Press, London, pp. 245–250.

Kasang, G., von Proff, L. and **Nicholls, M.** (1988) *Enzymatic conversion and degradation of sex pheromones in antennae of the male silkworm moth* Antheraea polyphemus. Z. Naturforsch., 43c, 275–284.

Keil, T.A. (1984) *Reconstruction and morphometry of silkmoth olfactory hairs: a comparative study of sensilla trichodea on the antennae of male* Antheraea polyphemus *and* Antheraea pernyi (*Insecta, Lepidoptera*). Zoomorphology, 104, 147–156.

Klein, U. (1987) *Sensillum-lymph proteins from antennal olfactory hairs of the moth* Antheraea polyphemus (*Saturniidae*). J. Insect Biochem., 17, 1193–1204.

Kodadová, B. (1996) *Resolution of pheromone pulses in receptor cells of* Antheraea polyphemus *at different temperatures.* J. Comp. Physiol. A, 179, 301–310.

Kumar, G. and **Keil, T.A.** (1996) *Pheromone stimulation induces cytoskeletal changes in olfactory dendrites of male silkmoths (Lepidoptera, Saturniidae, Bombycidae).* Naturwissenschaften, 83, 476–478.

Maida, R., Ziegelberger, G. and **Kaissling, K.E.** (1995) *Esterase activity in the olfactory sensilla of the silkmoth* Antheraea polyphemus. NeuroReport, 6, 822–824.

Manson, M.D., Boos, W., Bassford, P.J., Jr and **Rasmussen, B.A.** (1985) *Dependence of maltose transport and chemotaxis on the amount of maltose-binding protein.* J. Biol. Chem., 260, 9727–9733.

Meng, L.Z., Wu, C.H., Wicklein, M. and **Kaissling, K.E.** (1989) *Number and sensitivity of three types of pheromone receptor cells in* Antheraea pernyi *and* A. polyphemus. J. Comp. Physiol. A, 165, 139–146.

Pelosi, P. (1996) *Perireceptor events in olfaction.* J. Neurobiol., 30, 3–19.

Raming, K., Krieger, J. and **Breer, H.** (1989) *Molecular cloning of an insect pheromone-binding protein.* FEBS Lett., 356, 215–218.

Steinbrecht, R.A. (1973) *Der Feinbau olfaktorischer Sensillen des Seidenspinners (Insecta, Lepidoptera).* Z. Zellforsch., 139, 533–565.

Steinbrecht, R.A. (1992) *Stimulus transport and inactivation in insect olfactory sensilla-functional morphology, tracer experiments, and immunocytochemistry.* In Singh, R.N. (ed.), Neurobiology: Principles of Design and Function. Wiley Eastern, New Dehli, pp. 417–436.

Steinbrecht, R.A. (1997) *Pore structures in insect olfactory sensilla: a review of data and concepts*. J. Insect Morphol. Embryol., 26, 229–245.

Van den Berg, M.J. and **Ziegelberger, G.** (1991) *On the function of the pheromone binding protein in the olfactory hairs of* Antheraea polyphemus. J. Insect Physiol., 37, 79–85.

Vogt, R.G., Riddiford, L.M. and **Prestwich, G.D.** (1985) *Kinetic properties of a pheromone degrading enzyme: the sensillar esterase of* Antheraea polyphemus. Proc. Natl Acad. Sci. USA, 82, 8827–8831.

Vogt, R.G. and **Riddiford, L.M.** (1981) *Pheromone binding and inactivation by moth antennae.* Nature, 293, 161–163.

Vogt, R.G. and **Riddiford, L.M.** (1986) *Pheromone reception: a kinetic equilibrium.* In Payne, T.L., Birch, M.C. and Kennedy, C.E.J. (eds), Mechanisms in Insect Olfaction. Clarendon Press, Oxford, pp. 201–208.

Zack, C. (1979) Sensory adaptation in the sex pheromone receptor cells of saturniid moths. Diss. Fak. Biol. LMU München, pp. 1–99.

Ziegelberger, G. (1995) *Redox-shift of the pheromone-binding protein in the silkmoth* Antheraea polyphemus. Eur. J. Biochem., 232, 706–711.

Accepted on March 17, 1998